OPTIMIZATION OF ASYMMETRIC CROSS-SECTION OF SPARTAN SUPERWAY RAIL

FOR MINIMUM DISTORTION

A Project Presented to

The Faculty of the Department of

Mechanical Engineering

San Jose State University

In Partial Fulfillment

Of the Requirements for the Degree

Master of Science

in

Mechanical Engineering

by

Kriti Kalwad

May 2016

SAN JOSE STATE UNIVERSITY

The Undersigned Committee Approves

Optimization of the Asymmetric Cross-Section of the Spartan Superway Rail

For Minimum Distortion

Of

Kriti Kalwad

APPROVED FOR THE DEPARTMENT OF MECHANICAL ENGINEERING

_____

Dr. Raymond Yee, Committee Chair   Date

_____

Dr. Kedar Hardikar, Committee Member   Date

_____

Dr. Kurt McMullin, Committee Member   Date

ABSTRACT

Optimization of Asymmetric Cross-Section of the Spartan Superway Rail

For Minimum Distortion.

By Kriti Kalwad

There is an immediate need for transportation solutions that use renewable energy resources. Spartan Superway is a multi-year, multi-disciplinary project at San Jose State University seeking to create a sustainable personal rapid transport system for Silicon Valley. An overhead rail structure used in such a system for the purpose of the bogie wheels to roll over is that of great significance. A non-standard, asymmetric, braced, open cross-section is used for the Spartan Superway rail which needs thorough analysis to prove the working of the concept. This report summarizes the optimization process that can be carried out for the cross-section. The project used ANSYS as the finite element analysis software. The ANSYS finite element model was built and the results were validated with closed form solutions (where existent) and also with some preliminary experimental data. The slender, thin wall guiderail was best evaluated as a half-symmetric surface model with shell elements to make best use of the computational power at disposal. The FEA model and simulation procedure described can be used to accommodate and evaluate any future changes made to the design or constraints.

ACKNOWLEDGEMENTS

TABLE OF CONTENTS

NOMENCLATURE

CTW	Closed Thin Wall
OTW	Open Thin Wall
CFC	Closed Form Channel
C/S	Cross-Section
OD	Outer Diameter
CHS	Circular Hollow Section
RHS	Rectangular Hollow Section
SHS	Square Hollow Section
τ	Shear Stress
γ	Shear Strain
θ	Angle of twist
E	Elastic Modulus of material
G	Shear Modulus of material
I	Area moment of Inertia
J	Polar Moment of Inertia
T	Torque
D	Larger diameter
d	Smaller diameter
u	Circumferential displacement of strain probe

LIST OF TABLES

LIST OF FIGURES

x

1.0 INTRODUCTION

Spartan Superway:

The Spartan Superway [1] project is a multi-year and interdisciplinary project that is currently in its third year in an academic environment at San Jose State University. The Spartan Superway project is an effort to develop and demonstrate the technology of an Automated Transit Network (ATN) applied to a Personal Rapid Transit (PRT) system that is powered by solar energy.

Figure 1 – Sub-scale demonstration prototype of Spartan Superway

The motivation behind the Spartan Superway project is to eliminate major issues that plague personal mobility in dense urban areas such as:

- Traffic congestion
- Loss of productivity from time spent in commuting and/or parking
- Continued use of and dependence on hydrocarbon fuels
- Increased possibility of accidents that injure people and damage property
- Decrease in quality of life for residents (wasted time, increased stress, noise, smog)
- High cost of ownership for private vehicles, especially new 'green' vehicles, such as EVs
- Excessive consumption of raw materials in the production of automobiles
- Environmental degradation from greenhouse gas emissions and by products
- Inadequate mass transportation options (slow, limited service, and relatively high cost)

Spartan Superway aims to develop and bring to market the elements of a solar powered ATN system that will be scalable, replicable, and that can be located within existing rights of way in urban locales.

Figure 2 - Various design teams of Spartan Superway Project

Guideway Rail:

The concept representation of the structural system of Spartan Superway is seen below.
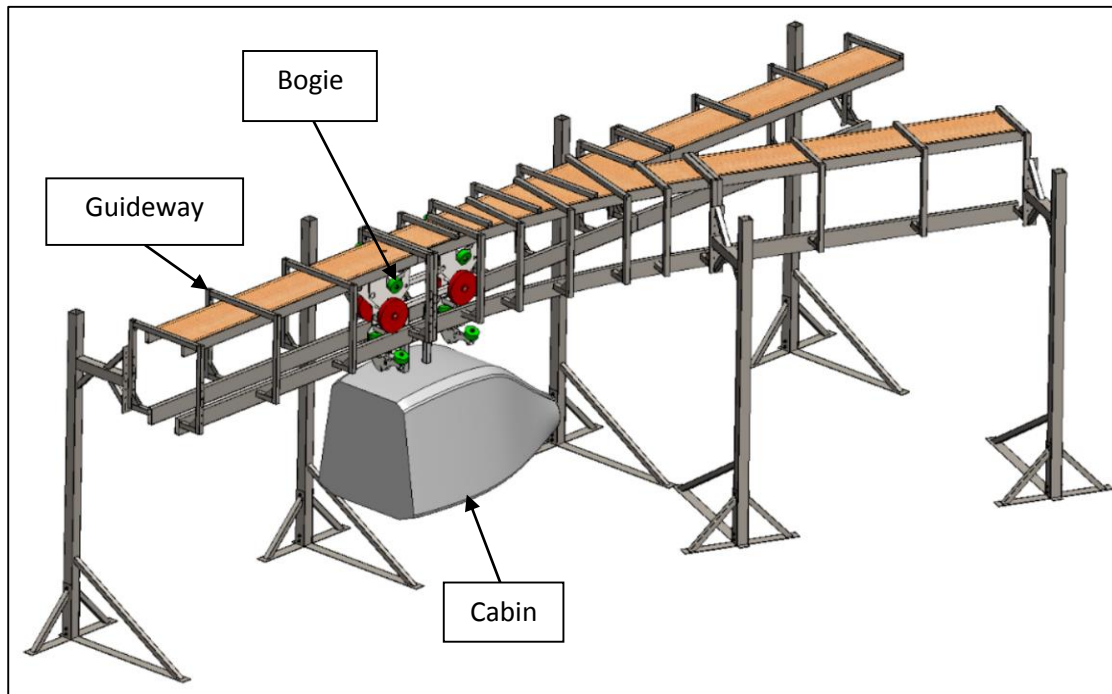
Figure 3 – Concept of Spartan Superway Structural System

The junction shown in Figure 3 above is that of a track-switch situation. The wheels of the bogie are automated to engage to only one side of the track in the direction that the cabin is meant to move towards. It is this track-switch junction that creates the asymmetric condition of the rail. The rail is to be designed for the worst loading conditions considered here.

At any other part of the guideway without the track-switch junction, the weight of the cabin+bogie is transferred through all 4 wheels of the bogie onto the rails present on either side.

The exact engagement of the bogie wheels onto the guideway rail is seen in the image below.

Figure 4 – Close-up of the Bogie on the Guideway system on the prototype

The current rail in the guideway system has been an adaptation of a concept by Bengt

Gustafsson, CEO Beamways AB, Sweden who is a consultant on the Spartan Superway panel.
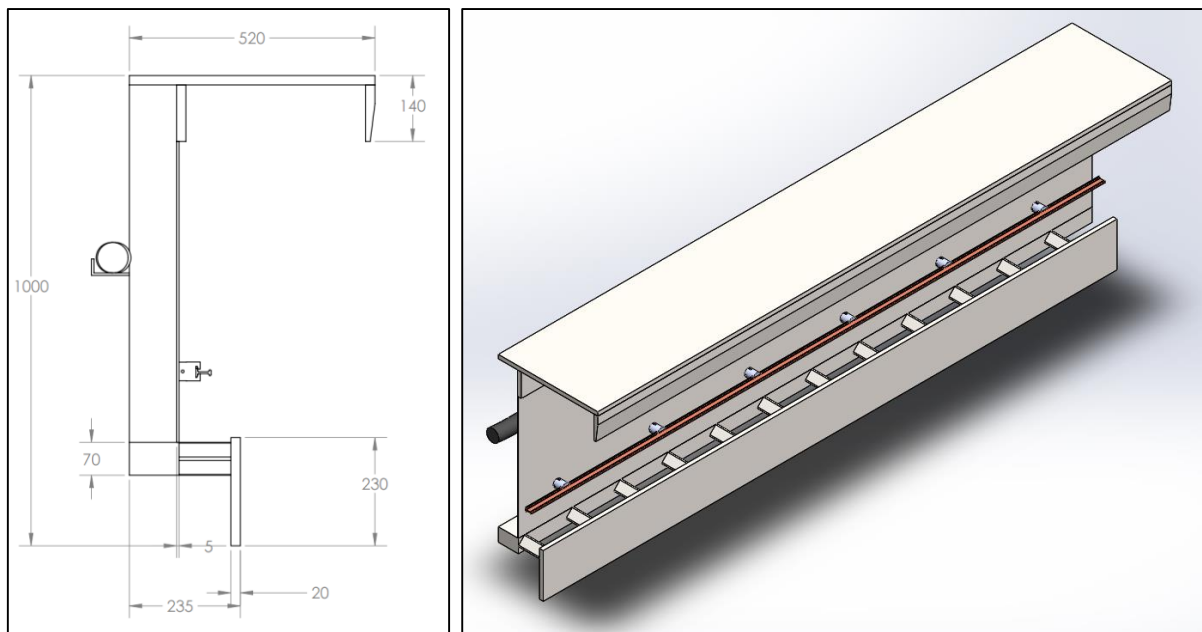
Figure 5 – Spartan Superway Rail cross-section as suggested by Beamways AB

This asymmetric cross-section is proposed to be fabricated by welding together steel plates and tubing for all lengths of the rail. At a track-switch junction as can be seen in Figure 2, when the bogie+cabin weighing upto 3,600 lbs hangs at the mid-span of the rail (40 ft from support) of the proposed 80 ft span while the other end is rigidly fixed to the support post and the next rail, the load does not act at the shear center of this cross-section. This implies that a point load results in bending as well as torsion of the rail. Therefore, torsional stiffness of this cross-section is of particular interest and is required to be assessed for the Spartan Superway guideway team.

The requirement of a minimum of 80 feet span for the rail, stems from cost analyses and urban aesthetic concerns. With other geometric constraints complying with various subsystems of Spartan Superway, the primary goal of the guideway team is to establish the optimal cross-section that is to be welded together for the entire length of the railway network. The author was consulted to carry out this optimization study. A full-scale model with real structural loading will be simulated using ANSYS and the cross-section dimensions for desired torsional stiffness using minimum material will be optimized for minimum deformation well within the elastic limit.

Modal and thermal analyses of the rail are also critical for finalizing the rail design. But, those analyses are beyond the scope of this project by the author.

1.1 Literature Review

A novel system such as the Spartan Superway is at the helm of setting industry standards for automated personal rapid transit systems. There are no exact American standards matching this system. Since this particular transportation system uses suspended cabin on rails, some existing standards such as ASME B30.11 (2010) - Monorails and Underhung Cranes and ANSI/ASCE/T&DI 21-13 - Automated People Mover Standards were referred to.

Several publications were found for lateral torsional buckling study of open thin wall (OTW) channels that were very relevant to the project. Since, the Spartan Superway rail is to be designed to lie well within the elastic limit, these papers at the very least provide thorough methodology ideas for study of OTW channels. Some of the publications and the key learnings from them are mentioned in the paragraphs to follow.

The paper by Put, Pi and Trahair (1999) [2] titled 'Bending and torsion of cold-formed channel beams', comprehensively compiled the behavior of cold-formed steel, OTW cross-sections under torsion. Both analytical and empirical methodologies followed in this paper to compare the effects of eccentricity and span on the torsional strength of beams provides key insights that can be applied to the Spartan Superway rail study. The paper reports the results of over 34 different bending and torsion tests carried out on unbraced simply supported cold-formed steel channel beams loaded eccentrically at mid-span. The paper concludes that beam strengths decrease as the load eccentricity increases and that the strength is higher when the load acts on the centroid side of the shear center than when it acts on the side away from the shear center. The effect of eccentricity on beam strength is higher than that of span.

A paper by Saadé, Espion and Warzée (2003) [3] titled 'Non-uniform torsional behavior and stability of thin-walled elastic beams with arbitrary cross sections.' compares the influence of non-uniform torsional warping on the linear behavior and the flexural torsional buckling of elastic thin-walled structures using different kinematic formulations. The complex governing equations of tension-compression, biaxial bending and non-uniform torsion have been uncoupled in this paper and the effects of the non-coincidence of the shear center and the centroid have been included in the study that provides a deeper insight into the complicated case of non-uniform torsion.

The paper by Gotluru, Shafer and Peköz (2000) [4] titled 'Torsion in thin-walled cold-formed steel beams.' also factors-in the partial warping restraint provided by various supports and sets up a method for an accurate closed form solution for a simple channel cross-section that is verified with finite element analysis.

A comprehensive body of work by Kavanagh and Ellifritt (1998) [5] titled 'Design Strengths of Cold-Formed Channels (CFCs) in Bending and Torsion.' concentrates on another important aspect of interest to the Spartan Superway rail, that of bracing. The cross-section is not a uniformly extruded section and is proposed to have equi-spaced bracing. The paper reports various tests of CFC beams loaded at the web centerline when symmetrically loaded and braced together in different arrangements. The results showed that the strengths of the CFCs generally increased as the amount of bracing increased.

A publication in the a conference proceeding by Zuberi , Kai and Zhengxing (2008) [6] titled 'Design optimization of Electric Overhead Travelling (EOT) Crane Bridge.' was insightful in its illustration of design optimization of a system with similar concerns as the Spartan Superway i.e., an overhead monorail system with a cabin, albeit, for a single operator. The publication lays out all the standards that are adhered to and sets up a clean method for design optimization in general of thin walled welded box girder subjected to rolling loads. The EOT optimal girder so designed is efficient in respect of design technique and verified as cost-effective. This study can be directly modified and applied to the optimization study of the Spartan Superway rail.

Several other papers were read by the author in the process of literature review to gain a thorough hold on the subject. General study of open thin wall (OTW) cross-sections from a textbook by Budynas[15] led the way to a simple, approximated hand calculation for an engineering judgment of the proposed cross-section.

1.2 Objective

The objective of the project is to optimize the dimensions of the Spartan Superway guideway rail cross-section for achieving minimum deformation with a suitable safety factor while using minimum material under static structural loading.

2.0 METHODOLOGY

2.1 Benchmark Case Analysis using ANSYS

In order to establish the relevance and accuracy of ANSYS as the suitable software for this

project, benchmarking the software is an important step. The ubiquity of the software at San Jose

State University also played a role in the choice of the software. Some relevant salient features of

ANSYS that are critical to the completion of the project are listed below.

- It is a robust finite element software with abundant technical support.

- It allows writing command line macros.

- It allows import of 3-D CAD model created using other software.

- Shell elements can be used for reducing analysis time of thin-wall members.

- There is a built-in, easy-to-use design optimization program.

A commonly available cross-section such as a circular hollow cross-section (pipe) rigidly

supported on one end and subjected to a torque on the other end was modeled and analyzed. The

results from ANSYS for maximum shear stress and angle of twist were then compared with

existing closed-form solutions, in order to verify the suitability of ANSYS.

The size of specimen and loading are not completely arbitrarily chosen. The torsion testing

machine available on campus with a 1000-10,000 N-m torque range was taken into

consideration. Commonly available strain gauges can read out strains of the order of 0.001. After

several iterations, a 0.6 m specimen of 2.5" OD and 0.25" thickness subjected to 1500 to 2000

N-m torque was chosen.

3-D All-quad elements were chosen for this analysis and mesh was refined until convergence was reached on strain energy values. Stress values were also compared for stability.
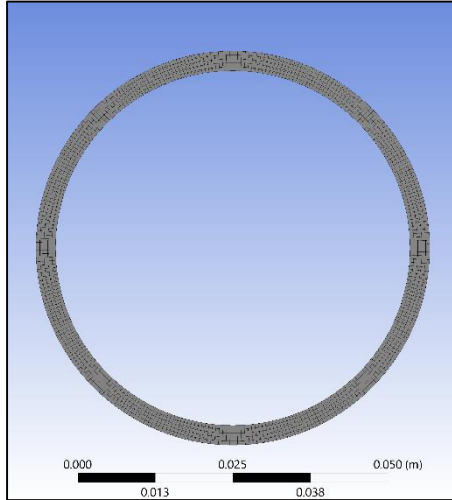
Figure 6 - Mesh with radially aligned elements
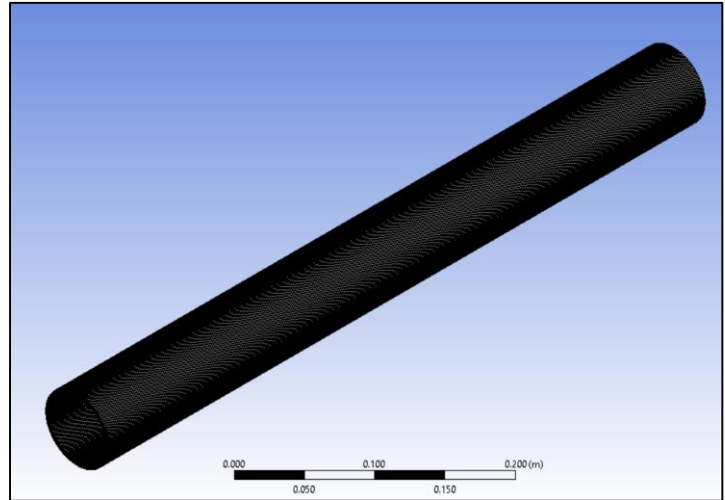
Figure 7 - Optimal mesh density for convergence
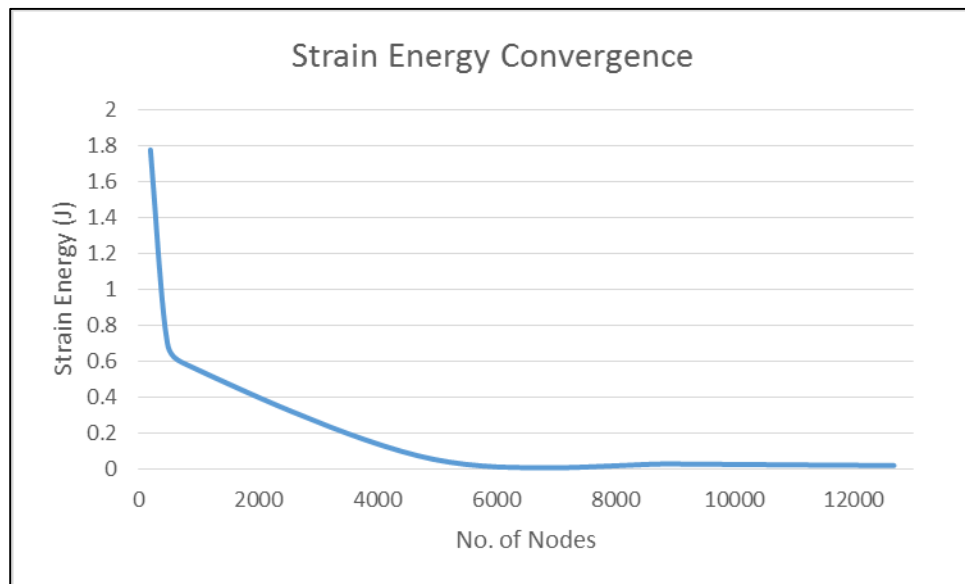
Figure 8 - Strain Energy vs No. of Nodes showing Convergence

The meshing was refined using sweep method and mapped-face mesh for arriving at optimum computational time. Finally, at element size of 60 µm there were 12680 nodes.

The specimen was given a fixed support on one end (A) and a moment of 1500 N-m (B) about Z-axis was applied on the other end as seen in Figure 9 below.
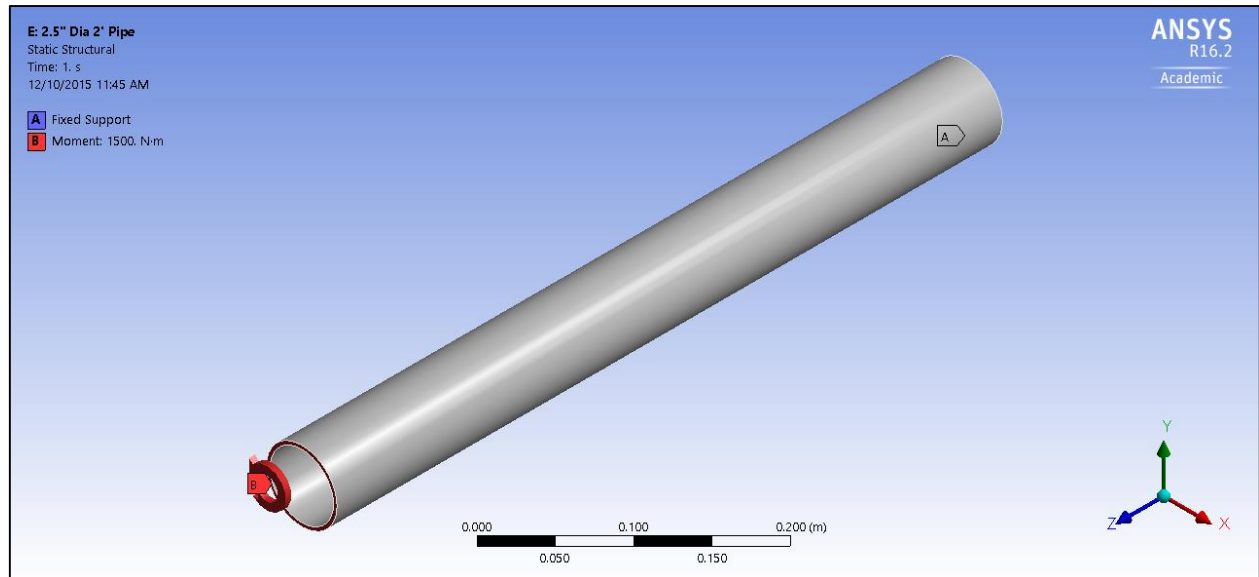
Figure 9 - Boundary Conditions in ANSYS

Figure 10 – Total deformation in the specimen

The total deformation was seen about Z-axis on the end where torque was applied as per expectations.

12

The maximum shear stress was observed on the outer face uniformly and was found to be

correctly varying along the thickness.
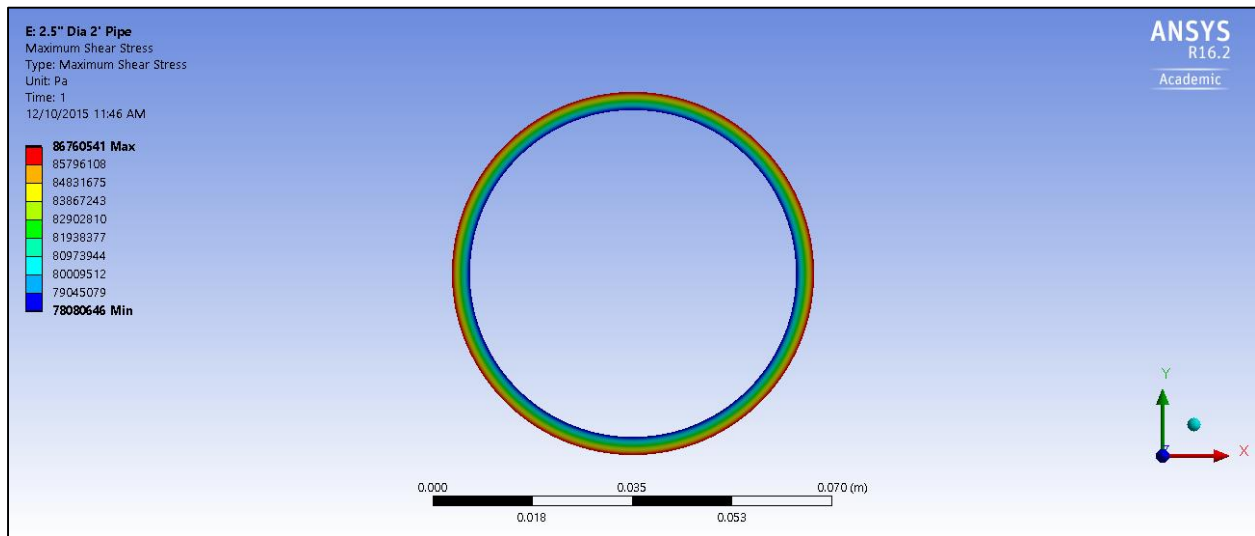
Figure 11 - Maximum Shear Stress in the specimen (C/S view)
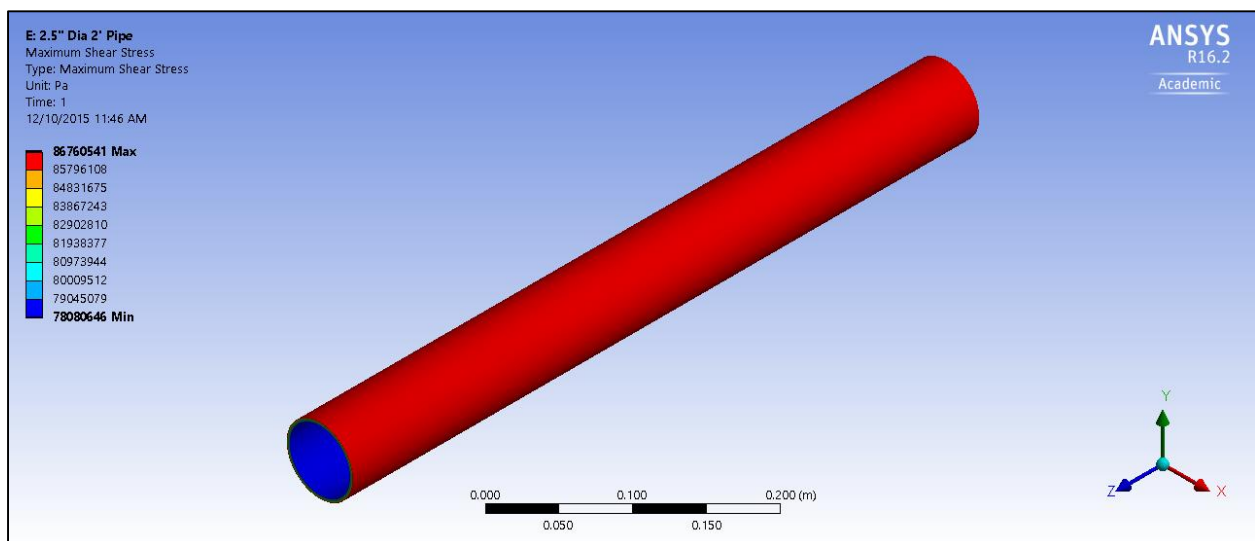
Figure 12 - Maximum Shear Stress in the specimen (ISO view)

The maximum shear strain (Figure 13) was observed as per expectations.
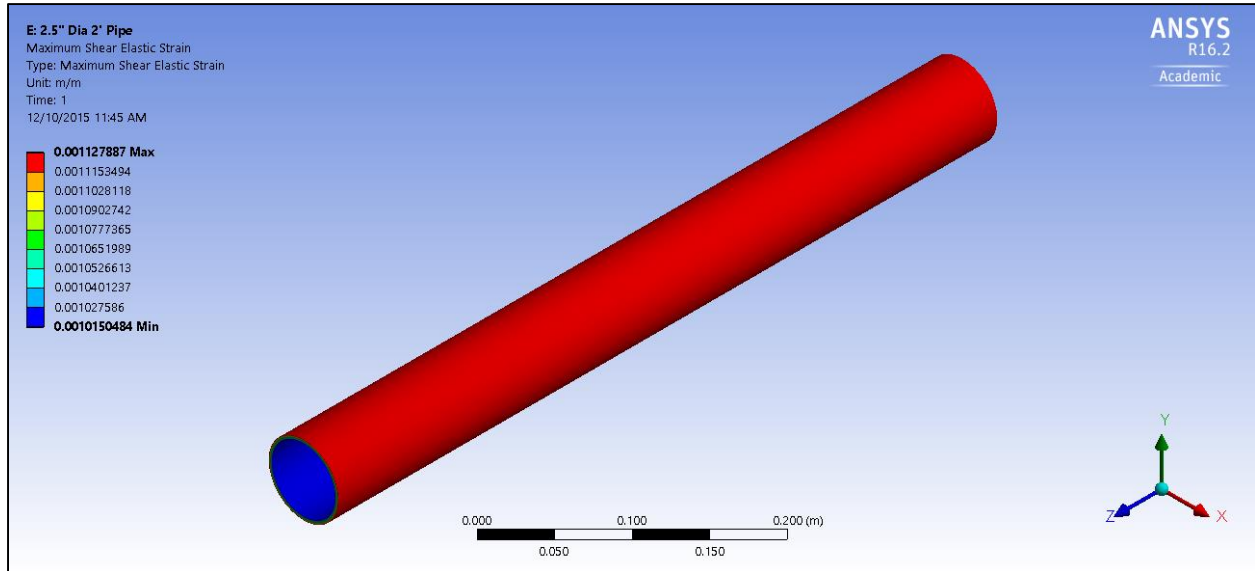
Figure 13 - Maximum Shear Strain in the specimen

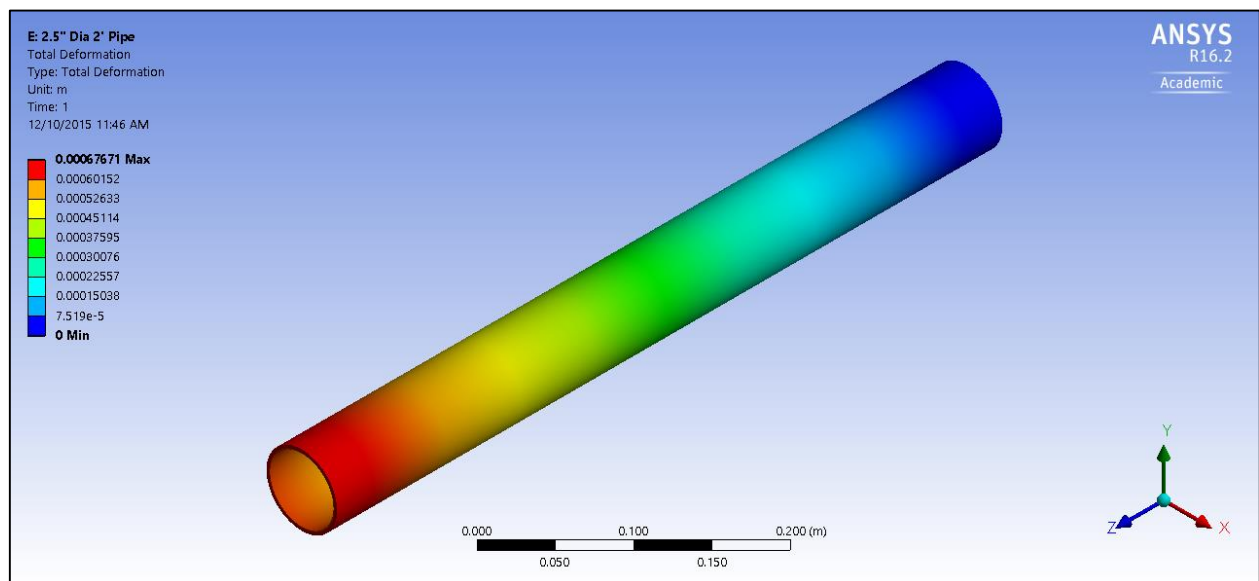The results are compared with the closed form solutions and are tabulated below in Table 1. For calculations of maximum shear stress and strain, see Appendix A.

Table 1 - Results Verification for 1500 N-m Torque

1500 N-m		Actual	ANSYS	% Difference
MPa	τ_{max}	86.758	86.761	**0.0038**
m/m	γ_{max}	0.00113	0.00113	**0.0454**
rad	θ	0.02075	0.02131	**2.7**

The same verification process was carried out for models applied with 1800 N-m and 2000 N-m as well. See Appendix B for results and verification tables. All results are in favor to conclude that ANSYS is a suitable software for this project.

14

Another important step in benchmarking ANSYS as a suitable and also feasible software to be used for the analysis was that of verifying accuracy of results with respect to processing time. For a thin walled slender specimen like the Spartan Superway Rail, a surface model meshed with shell element type can reduce processing time drastically while not compromising the solutions. This was verified initially with a simple 500mm long, 30mm equal angle (L-section) of 2mm thickness being treated as a solid body with solid elements and as a surface model with shell elements. The element size was fixed at 0.5mm edge length in both cases.

Statistics		Statistics	
Bodies	1	Bodies	1
Active Bodies	1	Active Bodies	1
Nodes	2219633	Nodes	117117
Elements	464000	Elements	116000

Figure 14 - Element statistics in Solid vs Surface models

The loads and constraints were as seen in Figure 15 below. One end of the specimen is rigidly held while a torque of 7000N-m is applied on the free end.
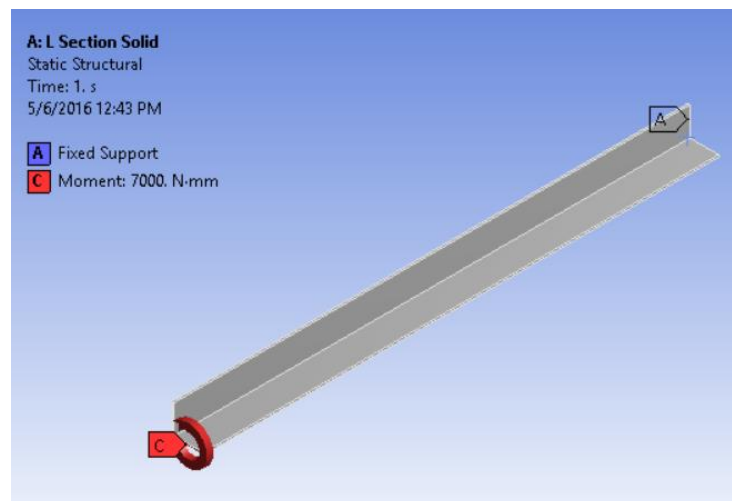

Figure 15 - Loads and Constraints on the L-Section

The difference in the processing power, time as well as solution file sizes in both cases are seen in Figure 16 below. While the model with solid elements took almost 15 times as long while consuming the maximum available memory, the shell elements solution was far simpler.

Details of "Solution (A6)"			Details of "Solution (A6)"		
Adaptive Mesh Refinement			**Adaptive Mesh Refinement**		
Max Refinement Loops	1.		Max Refinement Loops	1.	
Refinement Depth	2.		Refinement Depth	2.	
Information			**Information**		
Status	Done		Status	Done	
MAPDL Elapsed Time	8 m 58 s		MAPDL Elapsed Time	36. s	
MAPDL Memory Used	7.957 GB		MAPDL Memory Used	3.5693 GB	
MAPDL Result File Size	668.5 MB		MAPDL Result File Size	135. MB	
Post Processing			**Post Processing**		
Calculate Beam Section Results	No		Calculate Beam Section Results	No	

Figure 16 - Difference in processing power for Solid vs Surface model

When comparing deformation between these two models, it was about 6% higher in the surface model as seen in Figure 17 below.
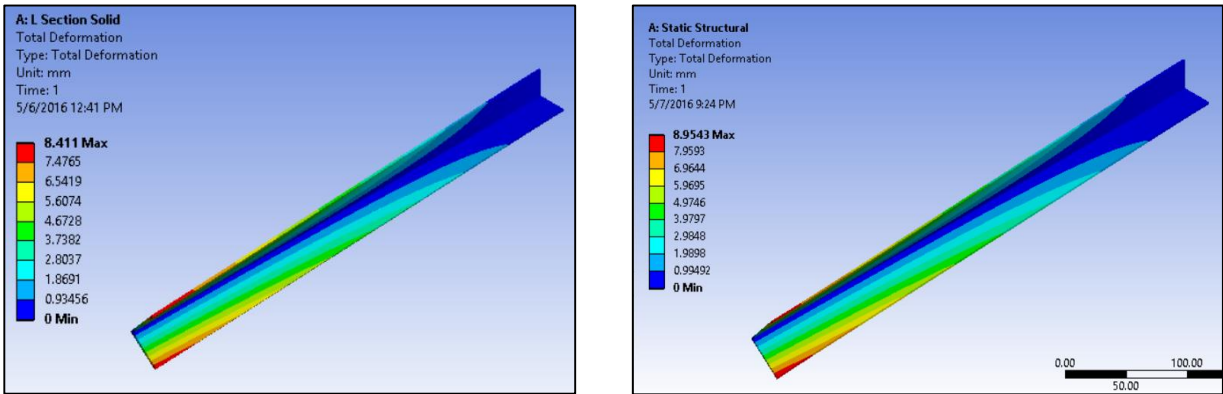

Figure 17 - Deformation in Solid vs Surface Model

This was consistent across loads and therefore, surface model proved to be a more viable option for the computing power at disposal.

2.2 Optimization of full-scale cross-section using ANSYS

The Spartan Superway system has several sub-systems that come in play with the rail components. Upon gathering of all finalized loading conditions and selection of suitable, cost-effective material for the rail, the analysis was then performed using ANSYS to check for the magnitude of deformation that it was going through.

The worst case conditions considered for the static-structural analysis is an event when all the cabins are halted one behind the other ("bumper-to-bumper") along the entire length of the rail. With an approximate outer dimension of the cabin being 12 ft, six cabins can be halted in a span of 80 ft (25m).
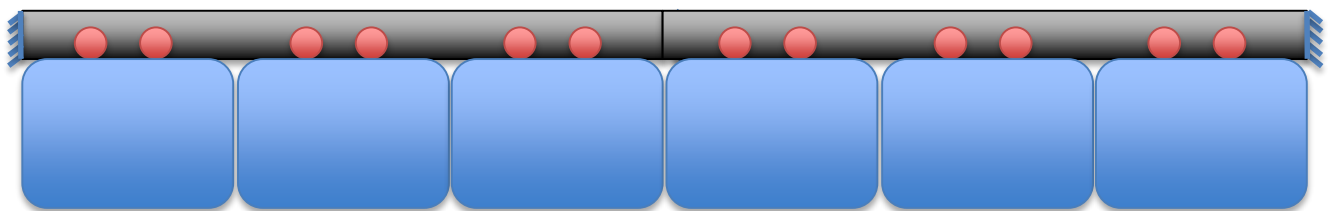

Figure 18 - Schematic of the worst load case condition

Since the plane of symmetry lies in the middle of the rail, a half-symmetric model can be used for FEA to reduce the processing time without compromising the results.
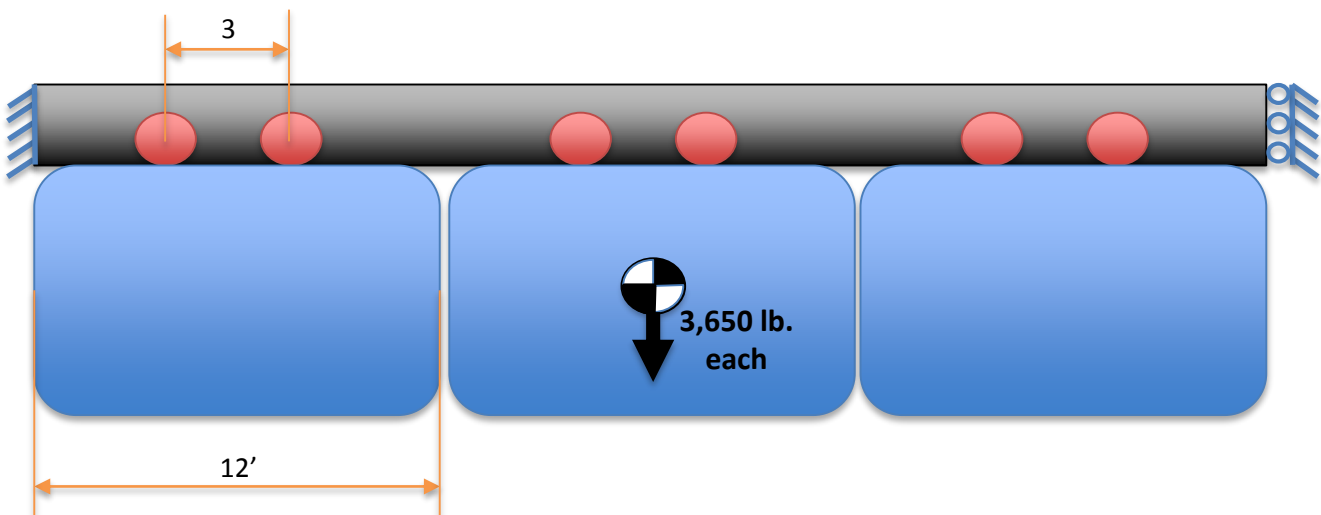
Figure 19 - Schematic of half-symmetric Model for FEA

17

The original design of the guiderail cross-section (See Fig 20) contains several solid components that could be replaced with hollow ones to reduce cost while not compromising on the desired minimum distortion and the corresponding stresses within safety. The optimization process was started with such replacements while deeming the outer dimensions as well as thicknesses of the replaced components as design variables to seek the desired goal.

The rails meant to carry the cables along the length of the guiderail are eliminated in order to simplify the model to only the structurally contributing members.
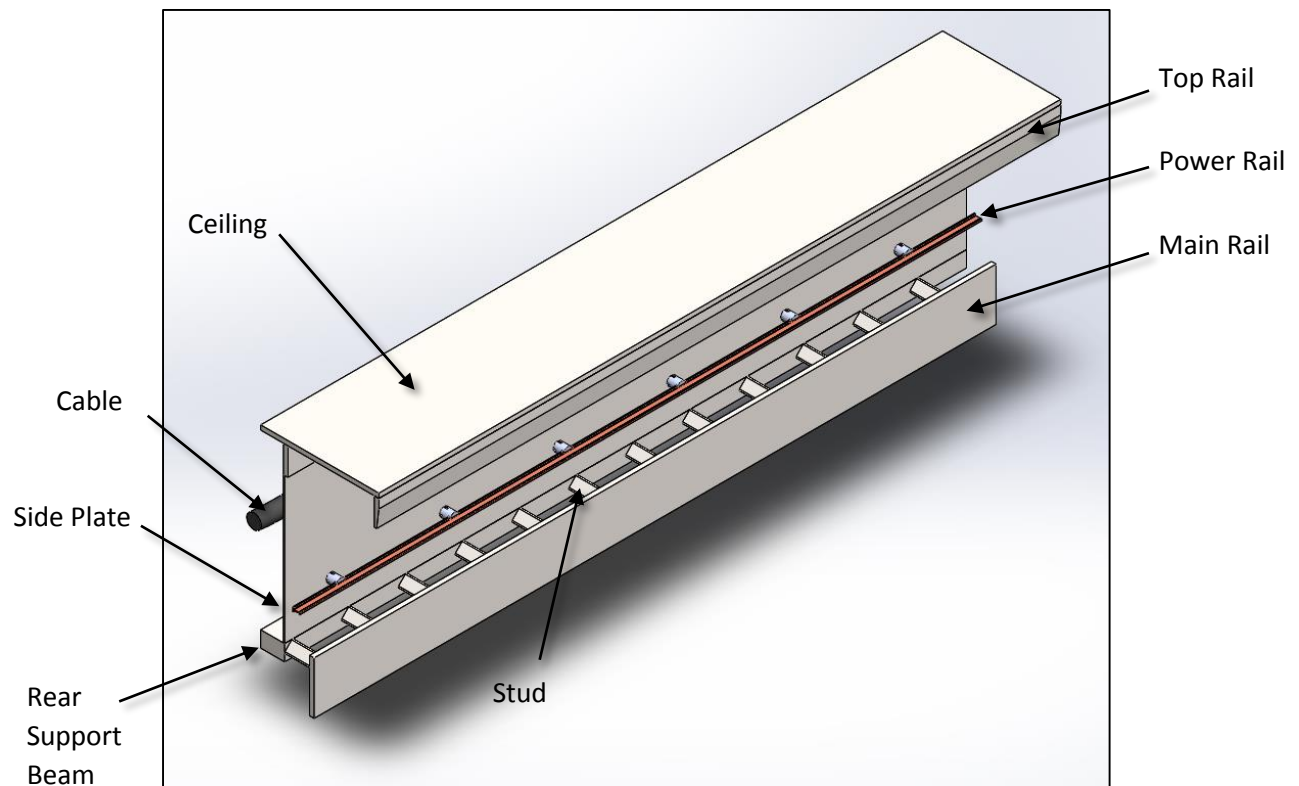
Figure 20 - Original guiderail cross-section design containing several solid components

A full scale model with symmetrical boundary conditions (12.5m long) was created with some changes to the design for cost reduction. The solid bar at the bottom rear of the rail as well as the solid studs were replaced with rectangular and square hollow sections respectively.
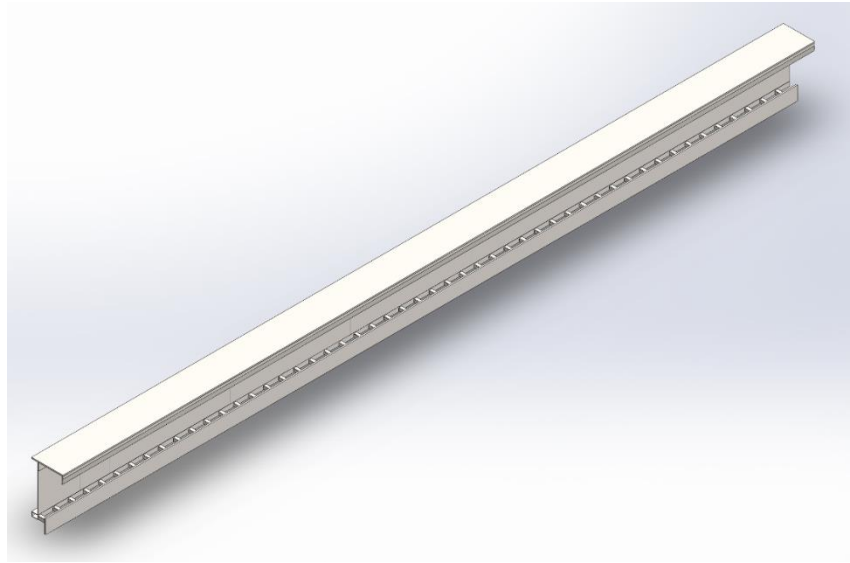
Figure 21 - Full scale symmetric model (12. 5m) of the simplified guiderail.
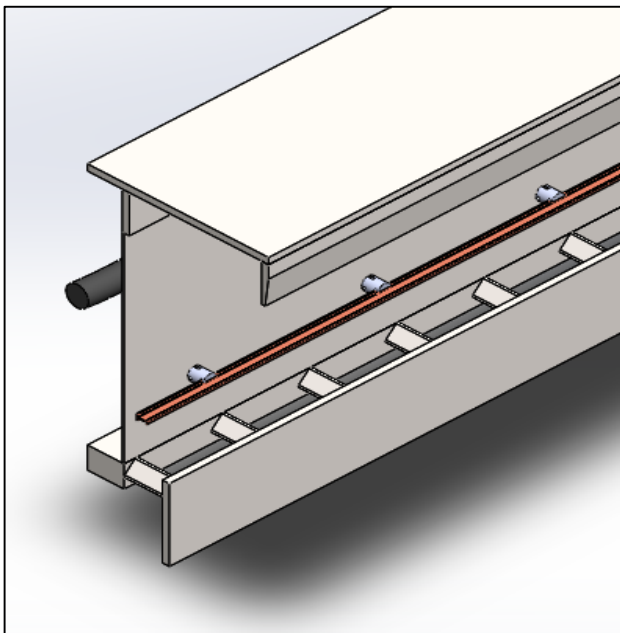
Figure 22 - Original cross-section.
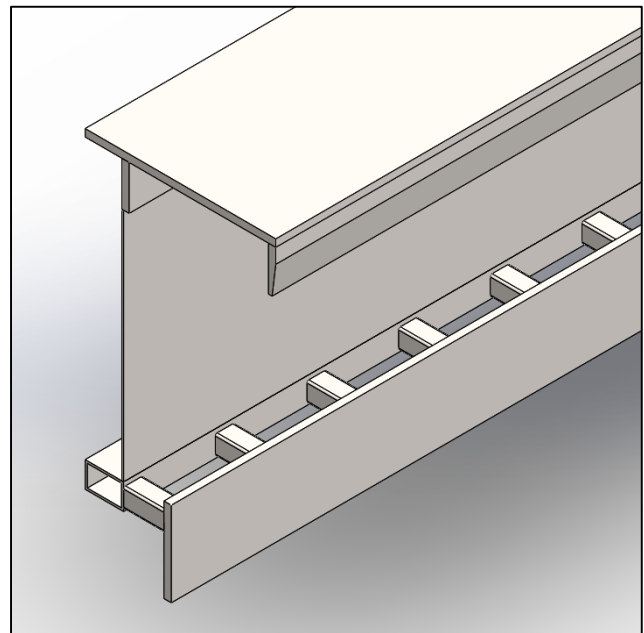
Figure 23 – Simplified cross-section.

The bottom-rear support beam was changed from a solid bar to a rectangular hollow section.
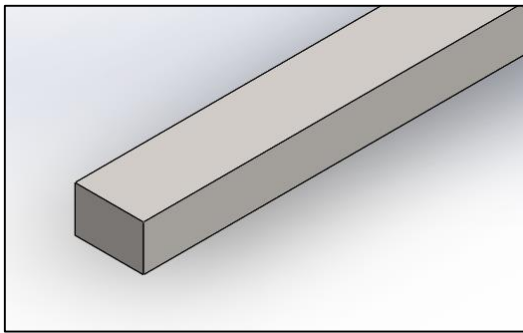
Figure 25 - Original bottom-rear support beam
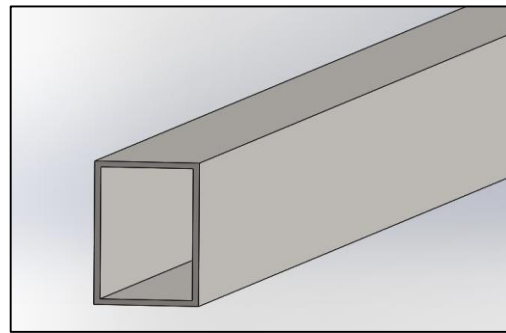
Figure 24 – Redesigned bottom-rear support beam.

The studs connecting the main rail to the side panels, were originally solid bars (meant to be bolted on diagonally). These were changed to hollow welded on options.
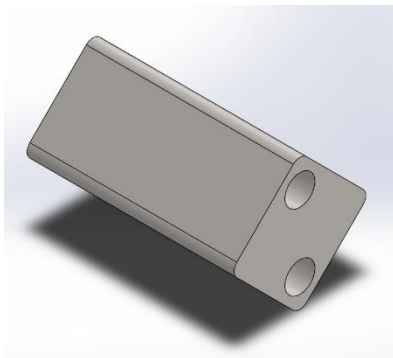
Figure 26 - Original bolt-on studs.
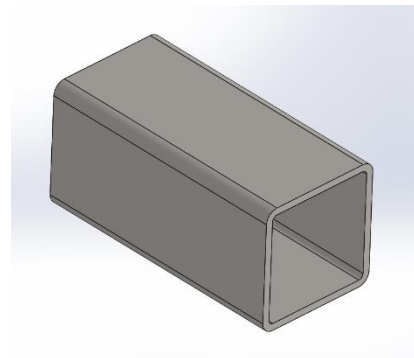
Figure 27 - Redesigned welded studs

One of the primary decisions that had to be made for the finite element analysis was that of solid elements vs shell elements for the specimen. For the available computational power at hand, the analysis was done using shell elements for faster, yet reliable simulation for carrying out optimization as well. See Appendix C for all the details of the model used in ANSYS for analysis.

The ideal way to begin with the finite element analysis is to model the guiderail in ANSYS Workbench. This allows for any and all dimensions of the components to be design parameters for optimization. An alternative method is to model it in a 3D CAD package such as Solidworks, ProE or NX and import an IGS file into the geometry part of the analysis settings.

The model used for illustration in this project is a simplified version purely to be used as an example rather than an actual sample. It was made in Solidworks. Mid-Surfaces were also extracted in SW and an IGS file containing all the surfaces extended and joined at all junctions was imported into ANSYS. All the thicknesses were specified and in this example, the side plate, rear support beam and the ceiling thicknesses were parametrized to illustrate the optimization process.
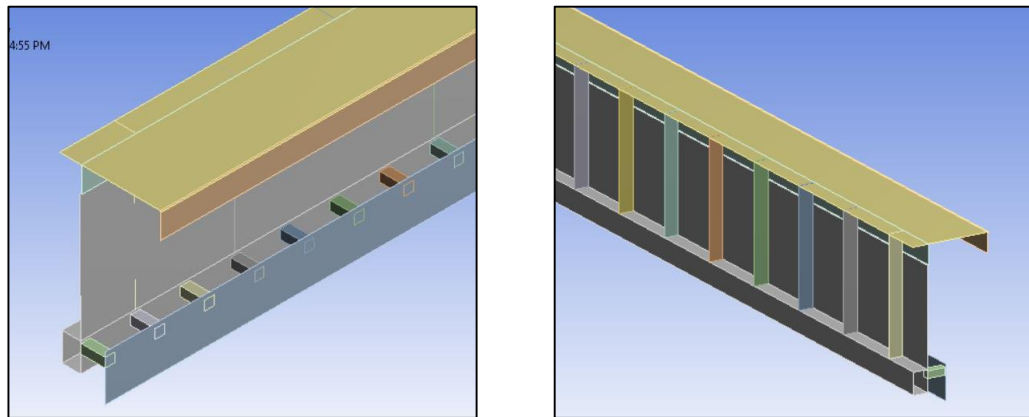
Figure 28 - Surface Model of the Spartan Superway guiderail

Meshing of the guiderail in this example was only refined to the point that the computer was capable of solving the analysis. This mesh definitely needs to be refined in order to achieve accurate results. One should comply by all the rules of a good mesh for the given body.
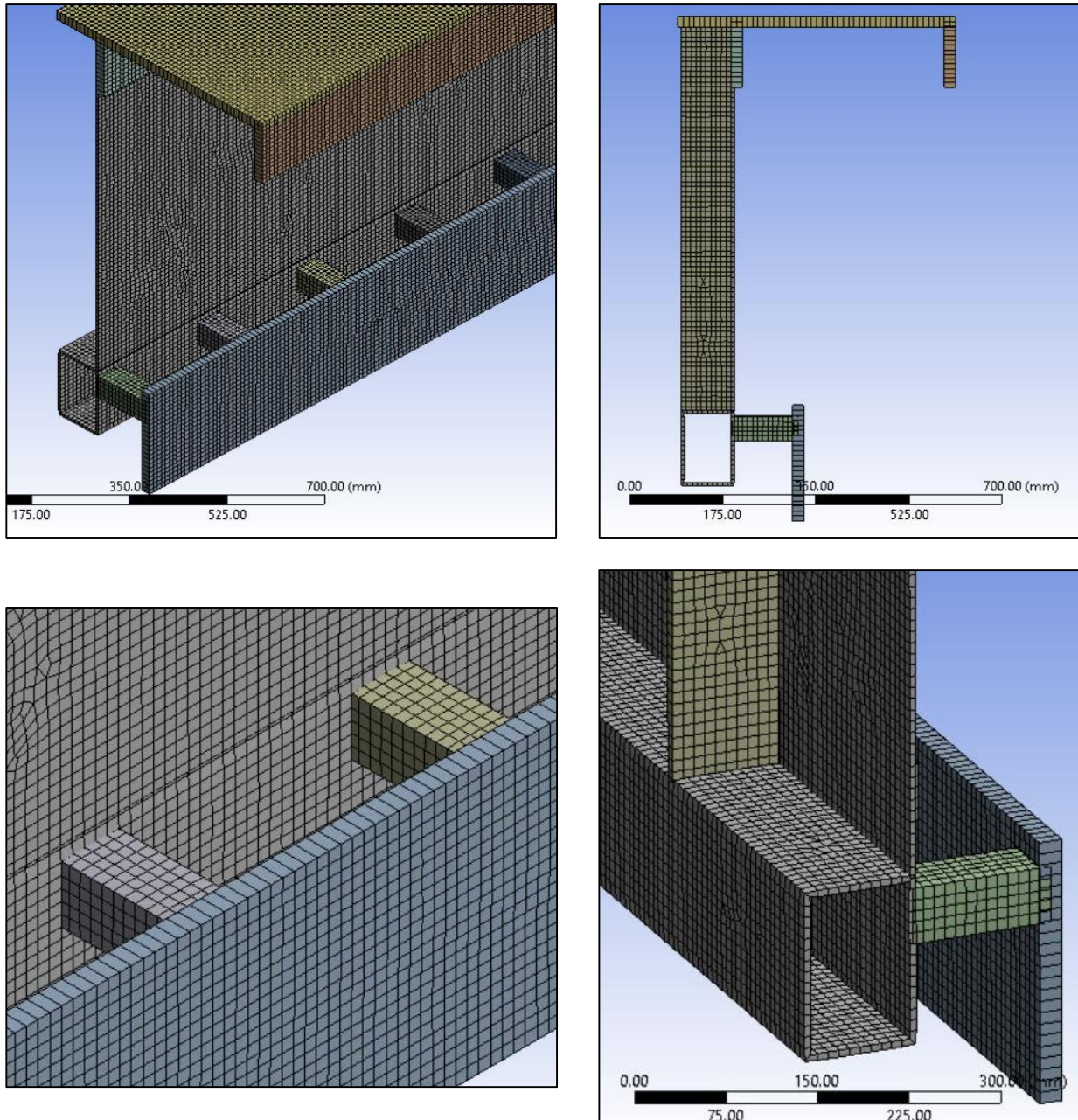
Figure 29 - Mesh details of the guiderail example in close-up view

The loads and constraints are specified in details earlier. A factor of 2 times the load is considered for sudden jerk/impact load. A FOS of 2 must be considered in determining the Max. Stress in the model.

(3650 x 0.45) Kg x 9.81 m/s^2 = 16200 N on 2 wheels. (Jerk Factor of 2 makes it 16200 N per wheel.)
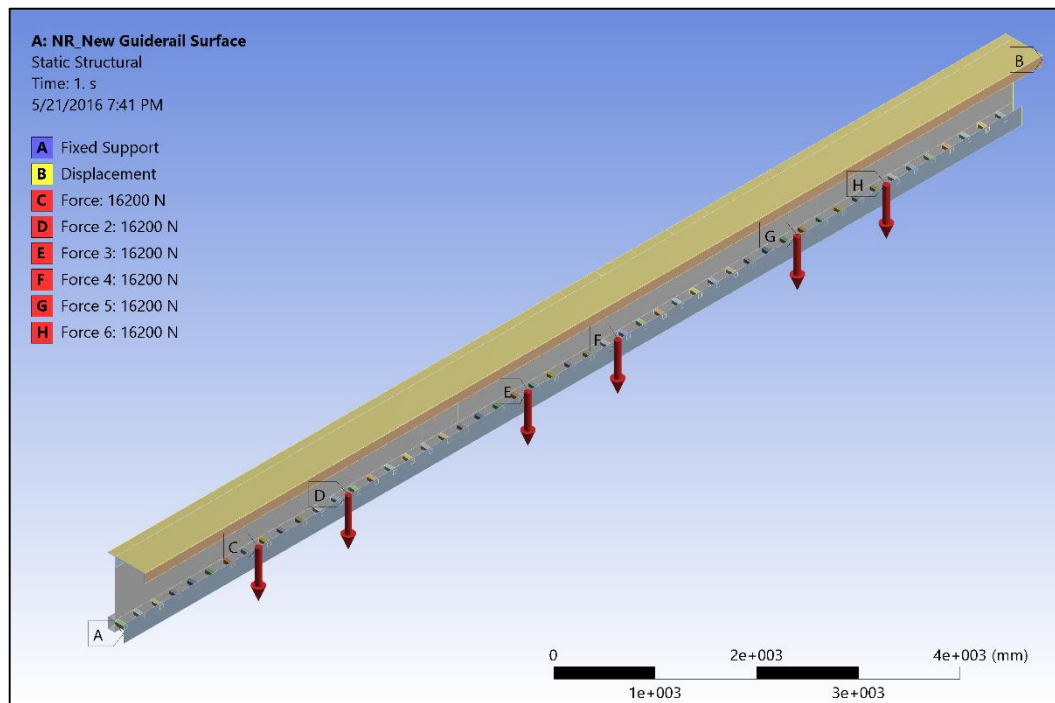
Figure 30 - Loads and Constraints in ANSYS

The design optimization parameters for this example run were chosen to seek 0<d<2mm deformation.
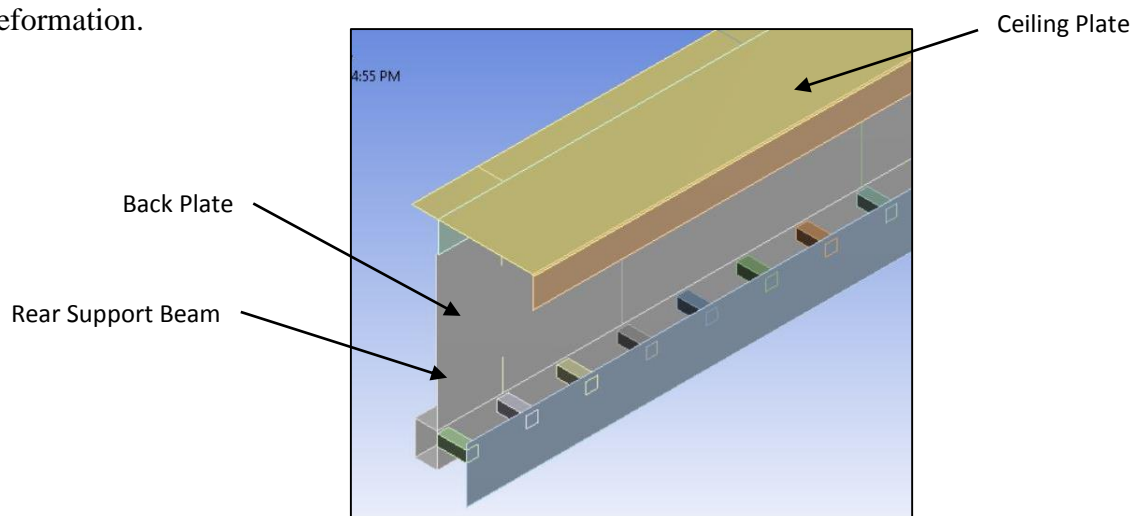
Figure 31 - Components of Guiderail for optimization

The optimization settings for this example run were as seen below. The thicknesses of the rear

support beam, ceiling and the side plate were set to vary (input parameters) and a deformation

goal was set.
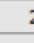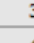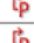
Outline of All Parameters		
	A	B
1	ID	Parameter Name
2	⊟ Input Parameters	
3	⊟ 🎞 NR_New Guiderail Surface (A1)	
4	🗗 P7	Rear Support beam Thickness
5	🗗 P8	Ceiling Thickness
6	🗗 P9	Side Plate Thickness
*	🗗 New input parameter	New name
8	⊟ Output Parameters	
9	⊟ 🎞 NR_New Guiderail Surface (A1)	
10	🗗 P3	Total Deformation Maximum
*	🗗 New output parameter	

Table of Schematic B2: Optimization							
	A	B	C	D	E	F	G
1			Objective		Constraint		
2	Name	Parameter	Type	Target	Type	Lower Bound	Upper Bound
3	Seek P3 = 0 mm; P3 <= 2 mm	P3 - Total Deformation Maximum	Seek Target ▼	0	Values <= Upper Bound ▼		2

Figure 32 - Optimization settings for example in ANSYS

2.3 Experimental Verification

A couple of torsion tests were conducted by the students in the Spartan Superway team with inputs from the author and other senior staff members of the team. (See Appendix D)

The primary objective of using these torsion test results was to benchmark the software. The first torsion experiment also served as a way for the Spartan Superway team members to familiarize themselves with the complexity of carrying out torsion test experiments, data acquisition from strain gauges and data interpretation thereafter.

2.4 Process documentation for future design changes

This project documents the simulation model, FEA results along with the ANSYS files included with this report serve as a future reference for any design changes that comes in the path of the Spartan Superway rail. The methodology defined in this project documentation, if used properly, will help any future design changes to be verified using ANSYS.

3.0 RESULTS AND DISCUSSION

The initial analysis run shows the max. deformation in mid-span as expected.
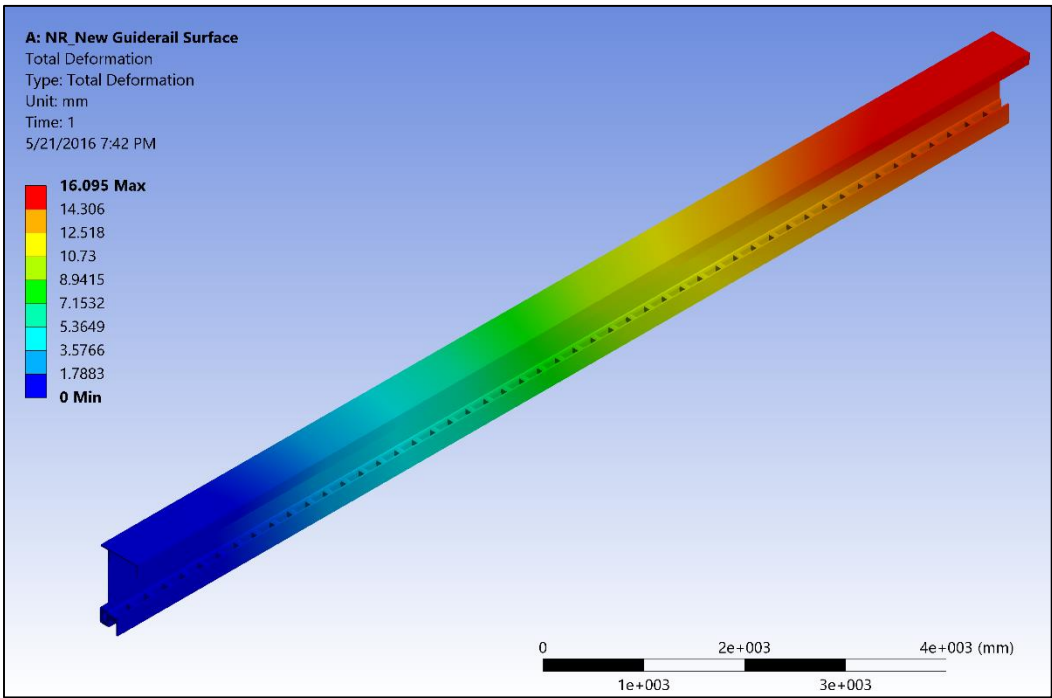
Figure 33 – Total deformation of guiderail

The individual deformation (in mm) in the X and the Y directions are shown separately below on the right plot.
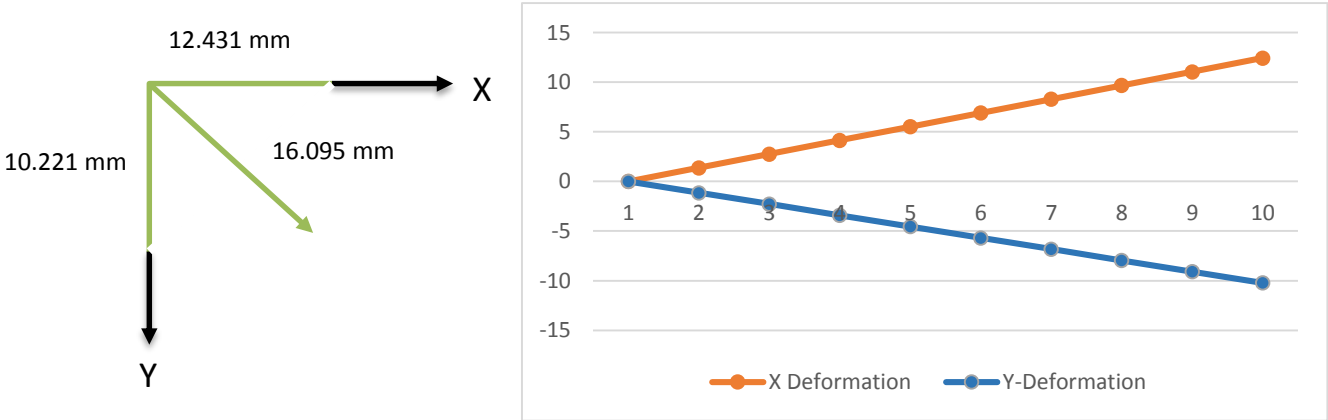
Figure 34 – Max. Total Deformation (left figure) and X, Y Deformation distributions along the rail

The results suggest that this is a case of biaxial bending. It appears that more bending deformation occurs in the X direction while Y direction bending is also of significant magnitude.

The example run optimization results are as seen below. For the given number of parameters, number of samples limited by the available computational power at the time of this study performed, the optimization process could not seek candidates for the target of less than 2mm deformation.
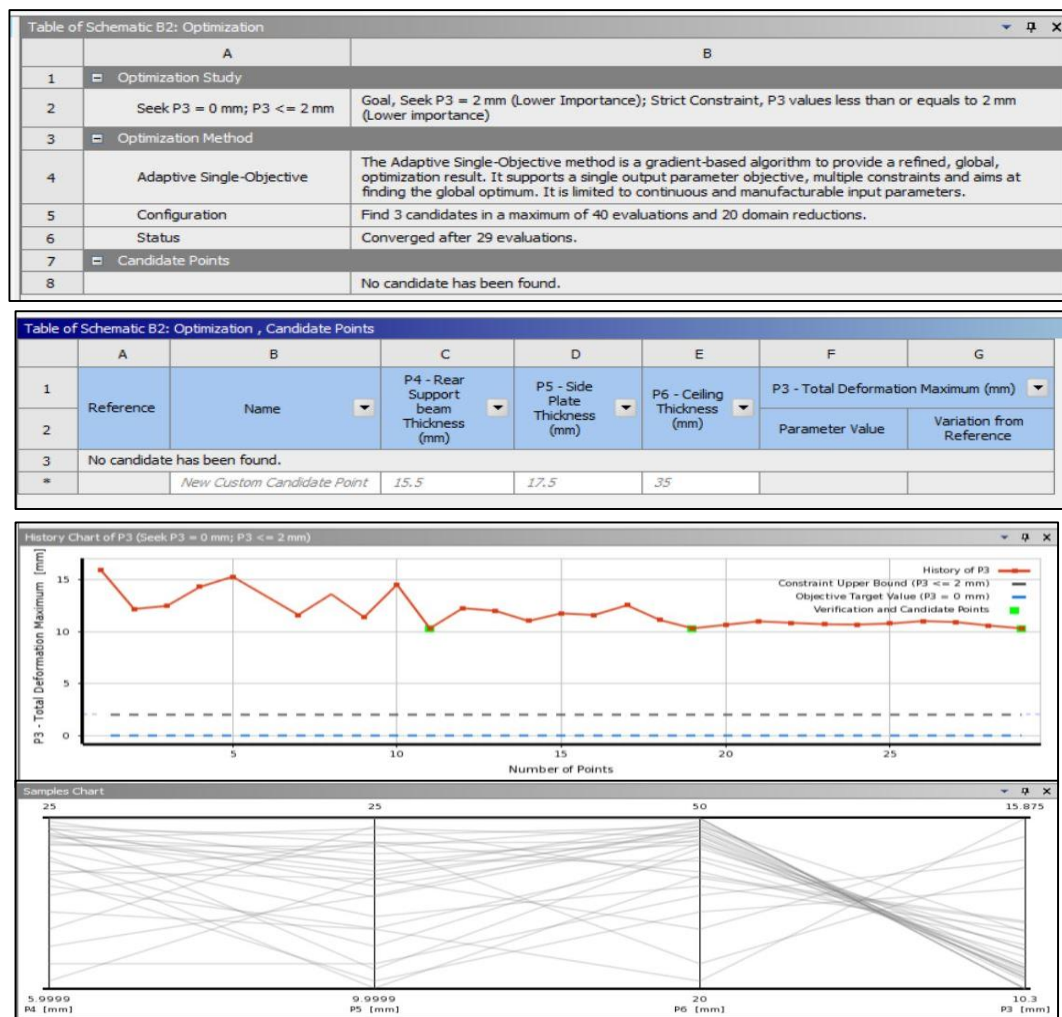
Figure 35 - Results Windows of Optimization

See Appendix E for all the values of all design points evaluated by the optimization runs.

The biaxial bending calls for a section modulus increase in both those directions to resist the undue deflections. One must also check angular displacement data to see the magnitude of torsional effect. Since, the maximum deflections occur primarily at mid-span, stiffening measures could be taken just around mid-span of the rail to minimize deflections while also making the design cost effective. This design choice can be made based on data from further analysis with a more refined mesh as the self-load of the rail (stiffeners away from the supported ends), could cause some more deflections.

Several design choices can and must be explored for optimizing the guiderail such as thicknesses and outer dimensions of various modifiable components. Spacing and dimensions of the bracing components such as the studs and the ribs at the back must also be parametrized in order to check for the effect they have on the overall stiffness.

4.0 CONCLUSIONS

The initial finite element analysis (with a coarse mesh) of the given model showed significant deformation in X and Y directions. This immediately hints at the fact that further reinforcements are necessary to resist the deflections.

The design optimization method outlined in this project can be used for further preliminary static structural analyses by others with basic understanding in FEA and ANSYS code knowledge.

The design optimization of the guiderail for Spartan Superway involves not just static structural analysis that is the topic covered in this project, but also modal and thermal analyses before arriving at the final cross-section fit for use.

The model used for this project is that of the straight portion of the guiderail. As expected, for turns, some portion of the guiderail will be curved in geometry. For those cases, separate analyses (structural, modal and thermal) must be carried out for the curved guiderail.

The static structural analysis carried out for this project was also limited by the computational resources at hand. Therefore, it must only be treated as a preliminary result for discussion. More design parameters such as outer dimensions and thicknesses of the various hollow components along with constraints (max. stress) and limiting factors (minimum material, etc.) must be specified and simulated with several samples for optimization to narrow down to suitable candidate points that can seek a suitable target of minimum deformation. A solid FEA model with 3D elements gives a more accurate solution and therefore is recommended to be studied for finalizing the cross-section dimensions.

REFERENCES

1. *Spartan Superway Project Info.* (n.d.). Retrieved Sept 1, 2015 from Spartan Superway
   Website:
   http://www.engr.sjsu.edu/smssv/projectInfo.html

2. Put, B. M., Pi, Y. L., & Trahair, N. S. (1999). Bending and torsion of cold-formed channel
   beams. *Journal of Structural Engineering*, *125*(5), 540-546.

3. Saadé, K., Espion, B., & Warzée, G. (2004). Non-uniform torsional behavior and stability of
   thin-walled elastic beams with arbitrary cross sections. *Thin-walled structures*, *42*(6), 857-
   881.

4. Gotluru, B. P., Schafer, B. W., & Peköz, T. (2000). Torsion in thin-walled cold-formed steel
   beams. *Thin-walled structures*, *37*(2), 127-145.

5. Kavanagh, K. T., & Ellifritt, D. S. (1994). Design strengths of cold-formed channels in
   bending and torsion. *Journal of Structural Engineering*, *120*(5), 1599-1607.

6. Zuberi, R. H., Kai, L., & Zhengxing, Z. (2008). Design optimization of EOT Crane
   Bridge. *Eng Opt*, 192-201.

7. Hu, Y., Jin, X., & Chen, B. (1996). A finite element model for static and dynamic analysis of
   thin-walled beams with asymmetric cross-sections. *Computers & structures*, *61*(5), 897-908.

8. Erkmen, R. E., & Mohareb, M. (2006). Torsion analysis of thin-walled beams including shear
   deformation effects. *Thin-walled structures*, *44*(10), 1096-1108.

9. Lin, W. Y., & Hsiao, K. M. (2003). More general expression for the torsional warping of a
   thin-walled open-section beam. *International journal of mechanical sciences*, *45*(5), 831-
   849.

10. Shakourzadeh, H., Guo, Y. Q., & Batoz, J. L. (1995). *A torsion bending element for thin-
    walled beams with open and closed cross sections*. Computers & Structures, *55*(6), 1045-
    1054.

11. Lau, S. C., & Hancock, G. J. (1987). Distortional buckling formulas for channel
    columns. *Journal of Structural Engineering*, *113*(5), 1063-1078.

12. Ronagh, H. R., Bradford, M. A., & Attard, M. M. (2000). Nonlinear analysis of thin-walled
    members of variable cross-section. Part I: Theory. *Computers & Structures*, *77*(3), 285-299.

13. Boswell, L. F., & Li, Q. (1995). Consideration of the relationships between torsion, distortion
    and warping of thin-walled beams. *Thin-walled structures*, *21*(2), 147-161.

14. Lee, J., & Lee, S. H. (2004). Flexural–torsional behavior of thin-walled composite
    beams. *Thin-Walled Structures*, *42*(9), 1293-1305.

15. Budynas, R. G. (1998). *Advanced strength and applied stress analysis*. McGraw-Hill
    Science/Engineering/Math.

16. Dowling, N. E. (1993). *Mechanical behavior of materials: engineering methods for deformation, fracture, and fatigue*. Prentice hall.

17. *INIST Library.* (n.d.). May 21, 2015. Retrieved Sept 1, 2015 from INIST Website: https://www.inist.org/library/2015-05-21.Ornellas%20et%20al.Spartan%20Superway%202014-2015%20Final%20Report.SJSU%20ME195.pdf

18. *Development and Construction of a Timber Composite Guide Way Beam and Steel Supporting Structure for a Full-Scale Prototype of an Elevated Transportation System by Keith McKenna* Sept 10, 2014. Retrieved Sept 1, 2015 from INIST Website: https://www.inist.org/library/2014-09-10.McKenna.Development%20and%20Construction%20of%20Guideway%20Beam.SJSU%20CE298.pdf

19. *Torsional Stress Evaluation of a potential cross-section for the Spartan Superway by Ka Yan Lau* April 14, 2015. Retrieved Sept 1, 2015 from email correspondence.

APPENDIX A – Shear Stresses And Torsional Constant Calculations

Maximum Shear Stress in a circular hollow section:

$$\tau_{max} = \frac{T\frac{D}{2}}{J}$$

Where

$$J = \frac{\pi(D^4 - d^4)}{32}$$

Maximum Shear Strain:

$$\gamma_{max} = \frac{\tau_{max}}{G}$$

Angle of Twist:

$$\theta = \frac{TL}{GJ}$$

Table 2 - Closed Form Solutions for the specimen

Units	Parameter		ANSYS		ANSYS		ANSYS
m	L	0.6		0.6		0.6	
Pa	G	7.90E+10		7.90E+10		7.90E+10	
m	D	0.0635		0.0635		0.0635	
m	d	0.05715		0.05715		0.05715	
N-m	T	1500		1800		2000	
m⁴	J	5.48943E-07		5.48943E-07		5.48943E-07	
MPa	τ_{max}	86.758	86.761	104.109	104.112	115.677	115.681
m/m	γ_{max}	0.001128399	0.001127887	0.001354079	0.001353406	0.001504532	0.001503849
m	u		0.00067671		0.00081205		0.00090228
rad	θ	0.020753361	0.021313701	0.024904034	0.025576378	0.027671148	0.028418268

APPENDIX B – Other ANSYS Results for Specimen
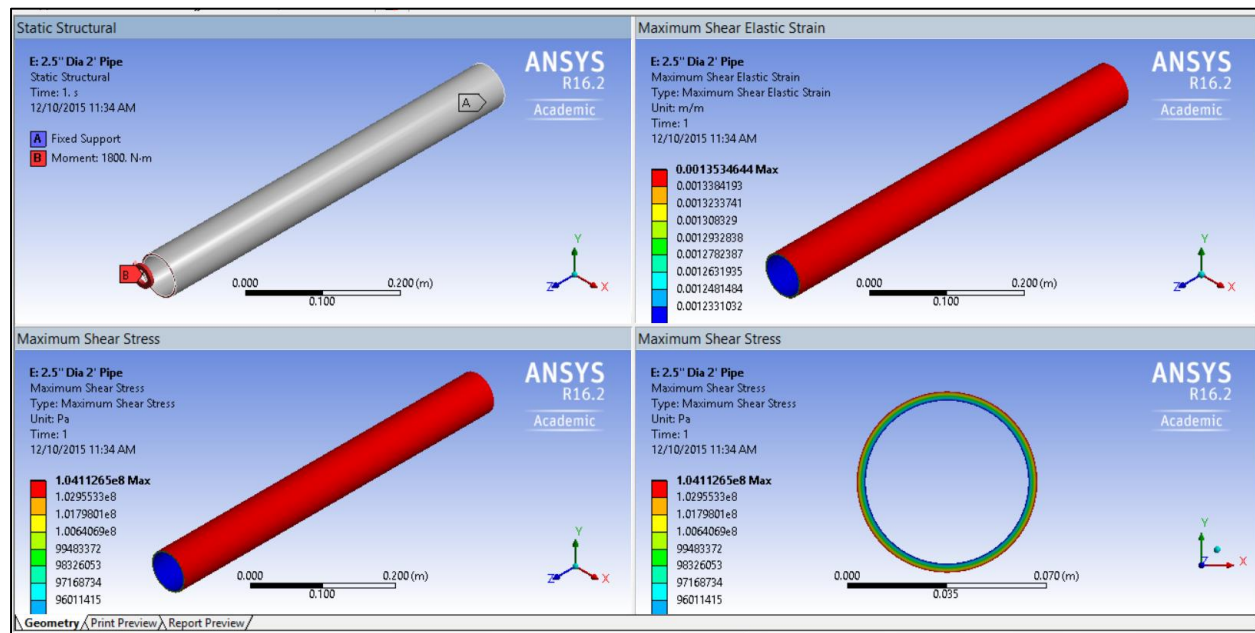
Figure 36 - Results for specimen subjected to 1800 N-m Torque
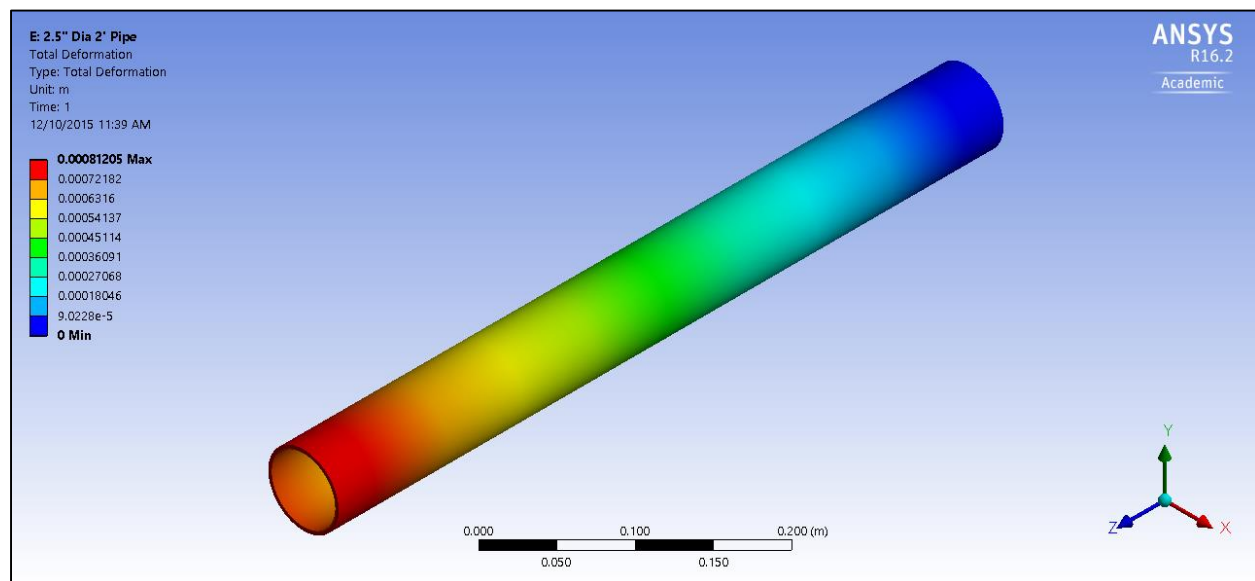
Figure 37 - Deformation for specimen subjected to 1800 N-m Torque
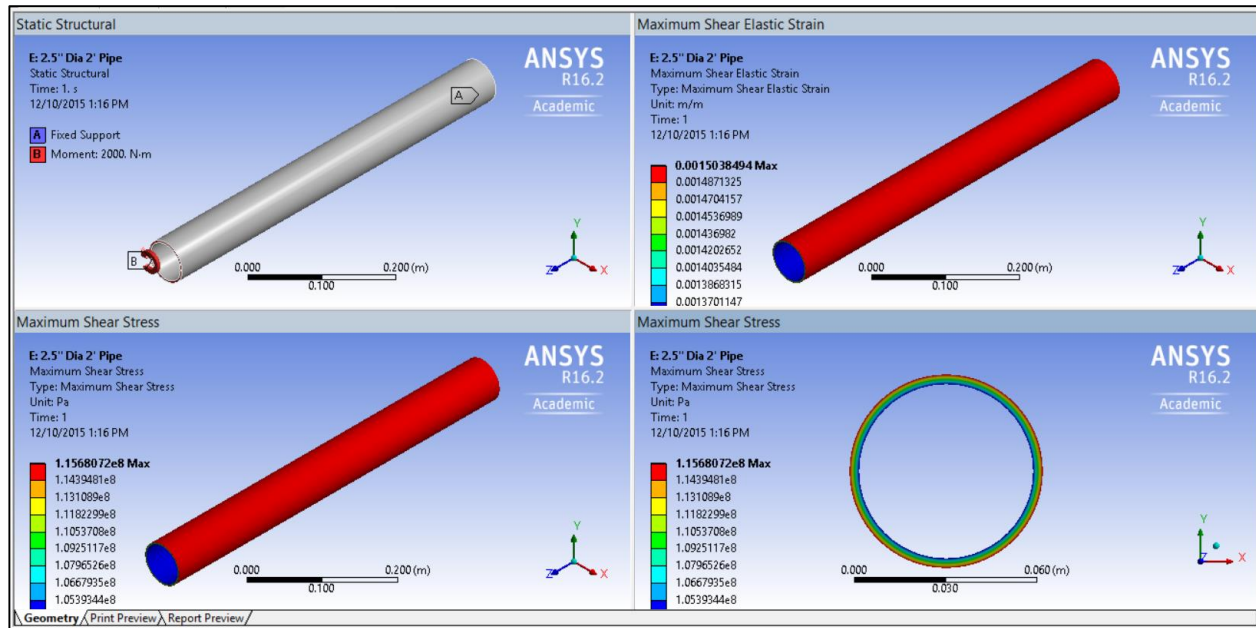
Figure 38 - Results for specimen subjected to 2000 N-m Torque
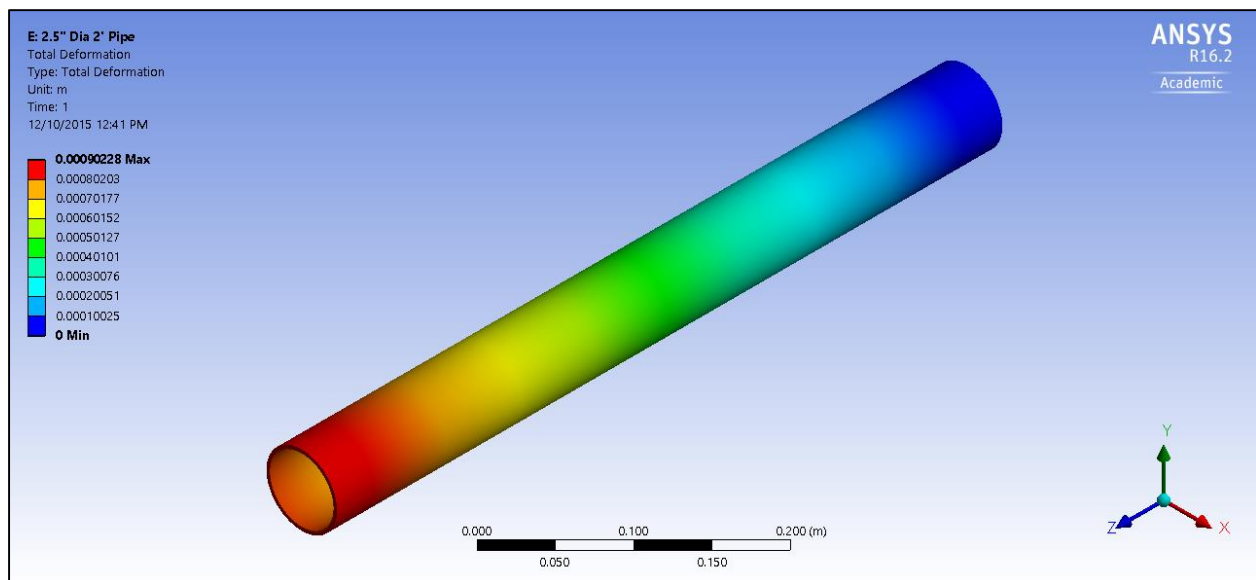
Figure 39 - Deformation for specimen subjected to 2000 N-m Torque

Table 3 - ANSYS vs Closed Form Solution Comparison

			1500	1800	2000	
MPa	**τ$_{max}$**	Actual	86.758	104.109	115.677	
		ANSYS	86.761	104.112	115.681	
		% Difference	0.0038	0.0027	0.0033	0.0032
m/m	**γ$_{max}$**	Actual	0.001128399	0.001354079	0.001504532	
		ANSYS	0.001127887	0.001353406	0.001503849	
		% Difference	0.0454	0.0497	0.0454	0.0468
rad	**θ**	Actual	0.020753361	0.024904034	0.027671148	
		ANSYS	0.021313701	0.025576378	0.028418268	
		% Difference	2.7000	2.6997	2.7000	2.6999
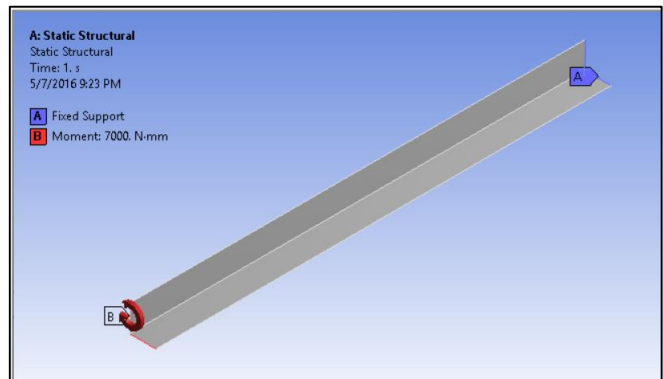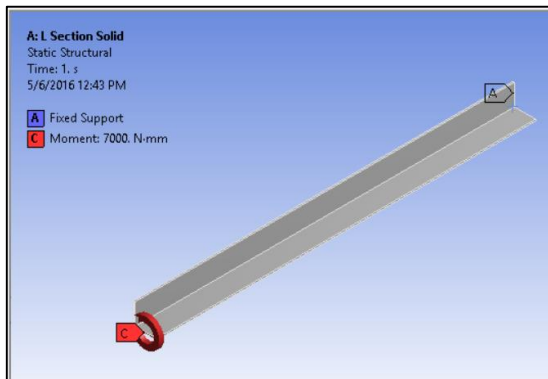
Figure 40 - L-Section Loads and Constraints (Solid vs Surface)
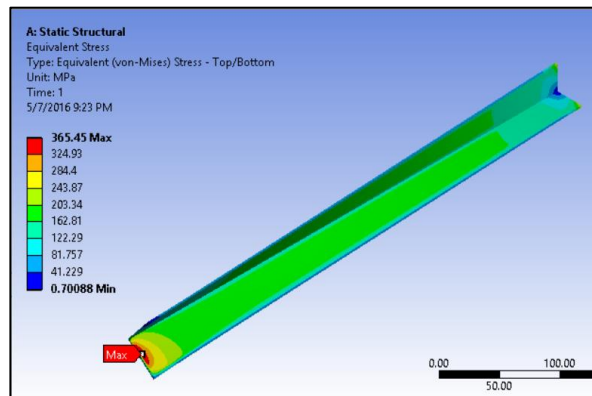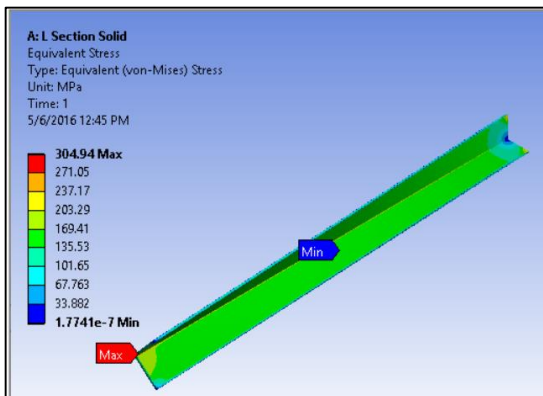
Figure 41 - Stresses in L-Section (Solid vs Surface)

35

APPENDIX C – FEA and Optimization Results for Guiderail

Table 4 - X and Y Deformation along rail

Location	Distance (m)	X Deformation (mm)	Y-Deformation (mm)
1	0.00	-0.0021643	0.00014887
2	1.39	1.3793	-1.1358
3	2.78	2.7607	-2.2718
4	4.17	4.1421	-3.4077
5	5.56	5.5235	-4.5437
6	6.94	6.9049	-5.6797
7	8.33	8.2863	-6.8156
8	9.72	9.6678	-7.9516
9	11.11	11.049	-9.0875
10	12.50	12.431	-10.223

Table of Schematic B2: Optimization

|	A	B	C	D	E
1	Name	P4 - Rear Support beam Thickness (mm)	P5 - Side Plate Thickness (mm)	P6 - Ceiling Thickness (mm)	P3 - Total Deformation Maximum (mm)
2	1	14.55	15.25	21.5	15.875
3	2	10.75	18.25	48.5	12.167
4	3	12.65	24.25	39.5	12.457
5	4	16.45	22.75	24.5	14.281
6	5	6.95	19.75	30.5	15.27
7	6	24.05	16.75	27.5	⚡x
8	7	20.25	13.75	45.5	11.596
9	8	18.35	10.75	33.5	13.592
10	9	22.15	21.25	42.5	11.373
11	10	8.85	12.25	36.5	14.509
12	11	25	25	50	10.3
13	12	21.343	16.369	38.052	12.243
14	13	17.434	15.313	43.253	11.986
15	14	23.116	18.051	46.897	11.012
16	15	18.668	22.904	40.633	11.743
17	16	23.824	11.73	44.744	11.588
18	17	20.692	10.137	39.896	12.522
19	18	19.089	19.684	47.926	11.104
20	19	25	25	50	10.3
21	20	23.305	20.328	49.409	10.645
22	21	23.952	19.056	46.281	10.977
23	22	24.162	22.823	45.77	10.837
24	23	24.606	20.907	47.844	10.697
25	24	21.988	22.499	48.984	10.667
26	25	22.673	24.088	46.788	10.764
27	26	22.915	21.878	45.24	11.005
28	27	22.467	20.008	47.355	10.908
29	28	23.74	23.512	48.41	10.574
30	29	25	25	50	10.3

Figure 42 - Design Points evaluated during Optimization

Figure 43 - Parameter variations during Optimization

APPENDIX D – Experimental Data

Following data is collected from Spartan Superway Guiderail Team:
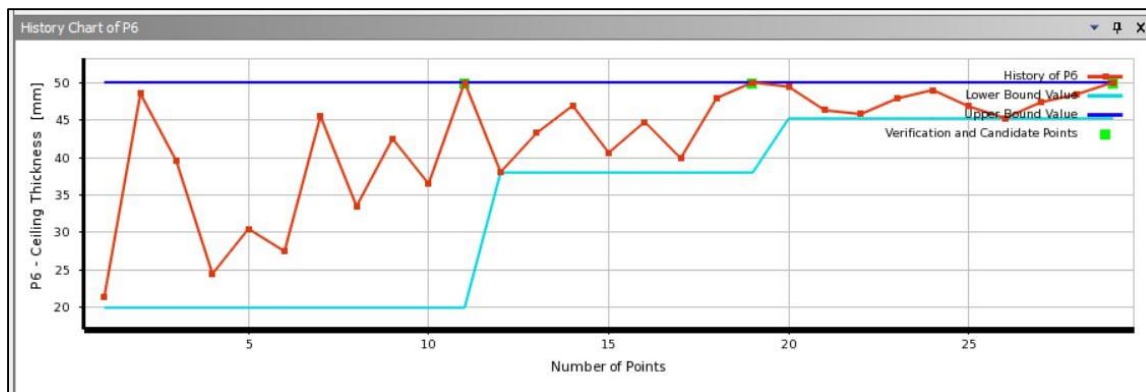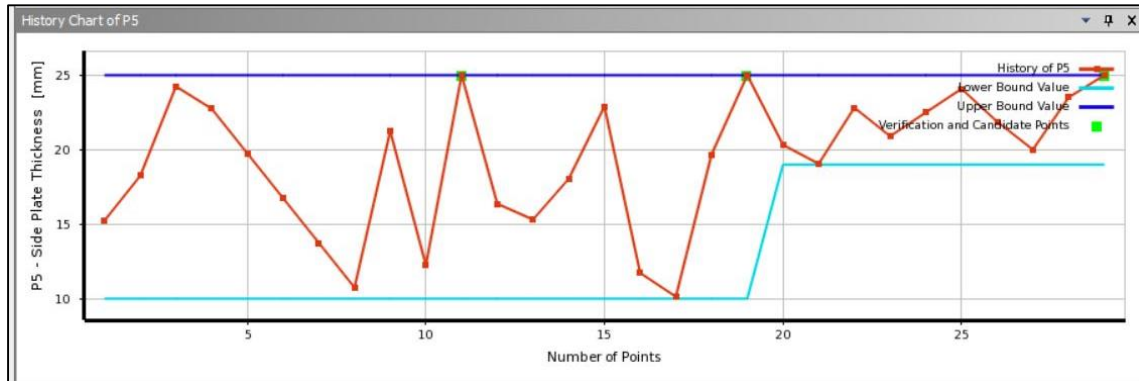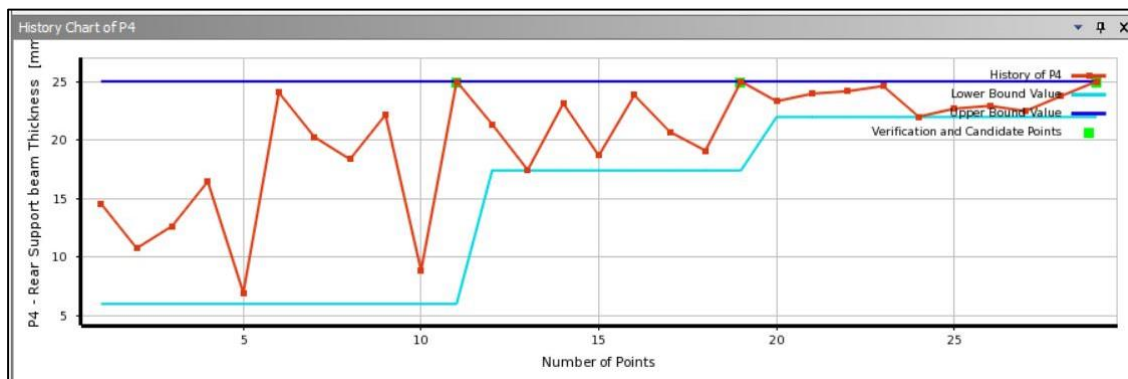
Table 5 - Experimental Data for Round Specimen 1

Torque (lb-in)	Left Angle (Degrees)	Right Angle (Degrees)	Angle of Twist (Degrees)	Calculated Angle (Degrees)	Percent Difference
750	0.6	1.1	0.5	0.26	63.16
1500	0.7	1.4	0.7	0.52	29.51
2250	0.9	1.8	0.9	0.78	14.29
3000	1.1	2.3	1.2	1.05	13.33
3750	1.4	2.9	1.5	1.31	13.52
4500	1.6	3.5	1.9	1.57	19.02
5250	1.8	4.1	2.3	1.83	22.76
6000	2.3	4.7	2.4	2.09	13.81
6750	2.5	5.2	2.7	2.35	13.86
7500	2.9	5.9	3	2.61	13.90
8250	3.3	6.6	3.3	2.87	13.94

Table 6 - Experimental Data for Round Specimen 2

Torque (lb-in)	Left Angle (Degrees)	Right Angle (Degrees)	Angle of Twist (Degrees)	Calculated Angle (Degrees)	Percent Difference
750	1.1	1.6	0.5	0.34	38.10
1500	1.3	2.1	0.8	0.67	17.69
2250	1.6	2.7	1.1	1.01	8.53
3000	1.8	3.3	1.5	1.35	10.53
3750	2.1	3.9	1.8	1.68	6.90
4500	2.4	4.5	2.1	2.02	3.88
5250	2.7	5.1	2.4	2.36	1.68
6000	3	5.7	2.7	2.69	0.37
6750	3.3	6.3	3	3.03	1.00
7500	3.6	7	3.4	3.36	1.18
8250	3.8	7.7	3.9	3.7	5.26

Table 7 - Angle of Twist Data for Round Specimen 3

Torque (lb-in)	Left Angle (Degrees)	Right Angle (Degrees)	Angle of Twist (Degrees)	Calculated Angle (Degrees)	Percent Difference
750	1.1	1.9	0.8	0.44	58.06
1500	1.6	2.8	1.2	0.88	30.77
2250	2.3	3.9	1.6	1.32	19.18
3000	2.7	4.8	2.1	1.75	18.18
3750	3.1	5.6	2.5	2.19	13.22
4500	3.4	6.4	3	2.63	13.14
5250	3.7	7.2	3.5	3.07	13.09
6000	4.2	8.1	3.9	3.51	10.53
6750	4.5	8.7	4.2	3.95	6.13
7500	4.9	9.6	4.7	4.39	6.82
8250	5.2	10.4	5.2	4.83	7.38

Table 8 - Shear Stress Data for Round Specimen 3

Torque (lb-in)	Measured shear strain from gauges - γ_{12}	ANSYS maximum shear strain - γ_{12}	Calculated maximum shear strain - γ_{12}	ANSYS % Difference from calculated	ANSYS % Difference from measured	Measured % Difference from calculated
750	1.940E-04	1.097E-04	1.106E-04	0.77	55.49	54.78
1500	3.110E-04	2.195E-04	2.212E-04	0.77	34.51	33.76
2250	4.660E-04	3.292E-04	3.317E-04	0.77	34.41	33.66
3000	5.980E-04	4.389E-04	4.423E-04	0.77	30.68	29.93
3750	7.370E-04	5.487E-04	5.529E-04	0.77	29.30	28.55
4500	8.720E-04	6.584E-04	6.635E-04	0.77	27.92	27.16
5250	9.990E-04	7.681E-04	7.740E-04	0.77	26.13	25.38
6000	1.144E-03	8.779E-04	8.846E-04	0.77	26.33	25.57
6750	1.274E-03	9.876E-04	9.952E-04	0.77	25.33	24.57
7500	1.408E-03	1.097E-03	1.106E-03	0.77	24.80	24.04
8250	1.541E-03	1.207E-03	1.216E-03	0.76	24.30	23.55

Table 9 - Shear Stress Data for Square Specimen

Torque (lb-in)	Measured shear strain from gauges - γ_{12}	ANSYS maximum shear strain - γ_{12}	ANSYS % Difference from measured
750	4.530E-04	9.000E-05	133.7016575
1500	5.640E-04	1.810E-04	102.8187919
2250	6.780E-04	2.710E-04	85.77449947
3000	7.900E-04	3.610E-04	74.54387489
3750	8.970E-04	4.520E-04	65.97479615
4500	1.005E-03	5.420E-04	59.85778927
5250	1.116E-03	6.320E-04	55.37757437
6000	1.231E-03	7.230E-04	51.99590583
6750	1.342E-03	8.130E-04	49.09512761
7500	1.453E-03	9.030E-04	46.6893039
8250	1.566E-03	9.940E-04	44.6875